

# Supplementary Information for

## PFPE-based polymeric $^{19}\text{F}$ MRI agents: a new class of contrast agents with outstanding sensitivity

*Authors:* Cheng Zhang,<sup>1,2</sup> Shehzahdi Shebbrin Moonshi,<sup>1,2</sup> Yanxiao Han,<sup>4</sup> Simon Puttick,<sup>1,2</sup> Hui Peng,<sup>1,2</sup> Bryan John Abel Magoling,<sup>1</sup> James C. Reid,<sup>1</sup> Stefano Bernardi,<sup>1</sup> Debra J. Bernhardt,<sup>1,3</sup> Petr Král<sup>4,5,6</sup> and Andrew K. Whittaker<sup>1,2\*</sup>

<sup>1</sup>Australian Institute for Bioengineering and Nanotechnology, The University of Queensland, Brisbane Qld 4072, Australia.

<sup>2</sup>ARC Centre of Excellence in Convergent Bio-Nano Science and Technology

<sup>3</sup>School of Chemistry and Molecular Biosciences, The University of Queensland, Brisbane Qld 4072, Australia.

<sup>4</sup> Department of Chemistry, University of Illinois at Chicago, Chicago, Illinois 60607, USA.

<sup>5</sup> Department of Physics, University of Illinois at Chicago, Chicago, Illinois 60607, USA.

<sup>6</sup> Department of Biopharmaceutical Sciences, University of Illinois at Chicago, Chicago, Illinois 60612, USA.

\*E-mail: [a.whittaker@uq.edu.au](mailto:a.whittaker@uq.edu.au)

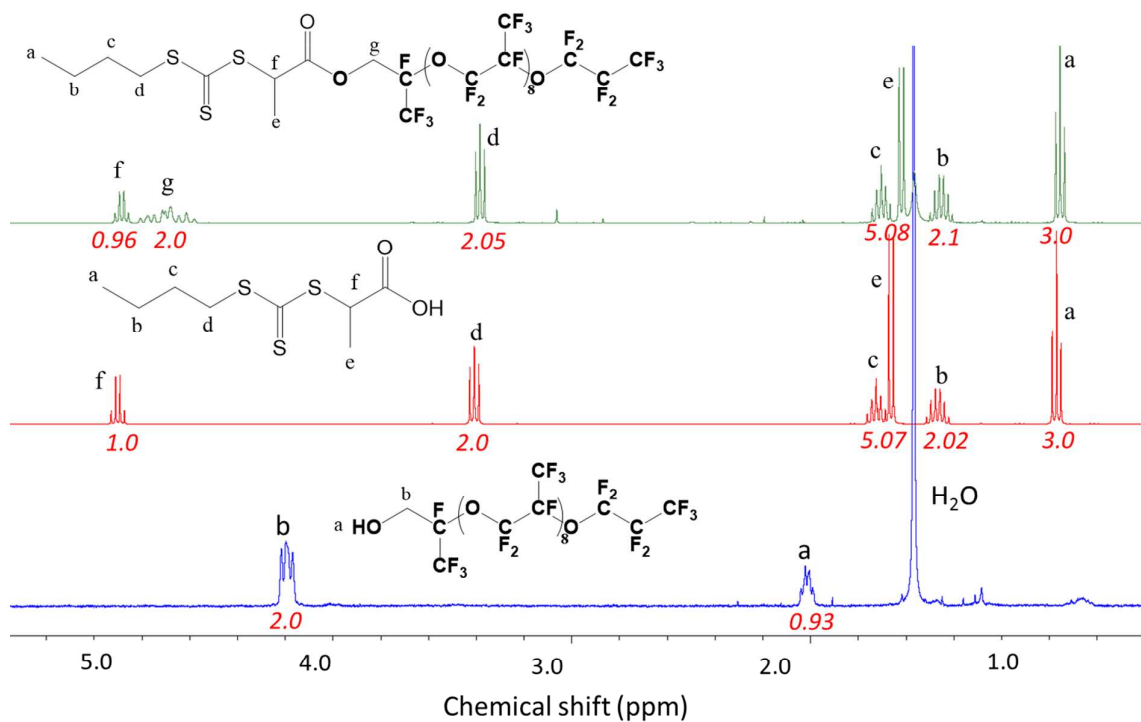


**Figure S1.** The  $^1\text{H}$  NMR spectra of PFPE-OH (bottom), PABTC (middle) and PABTC-PFPE macro-CTA (top) in  $\text{CDCl}_3$ .

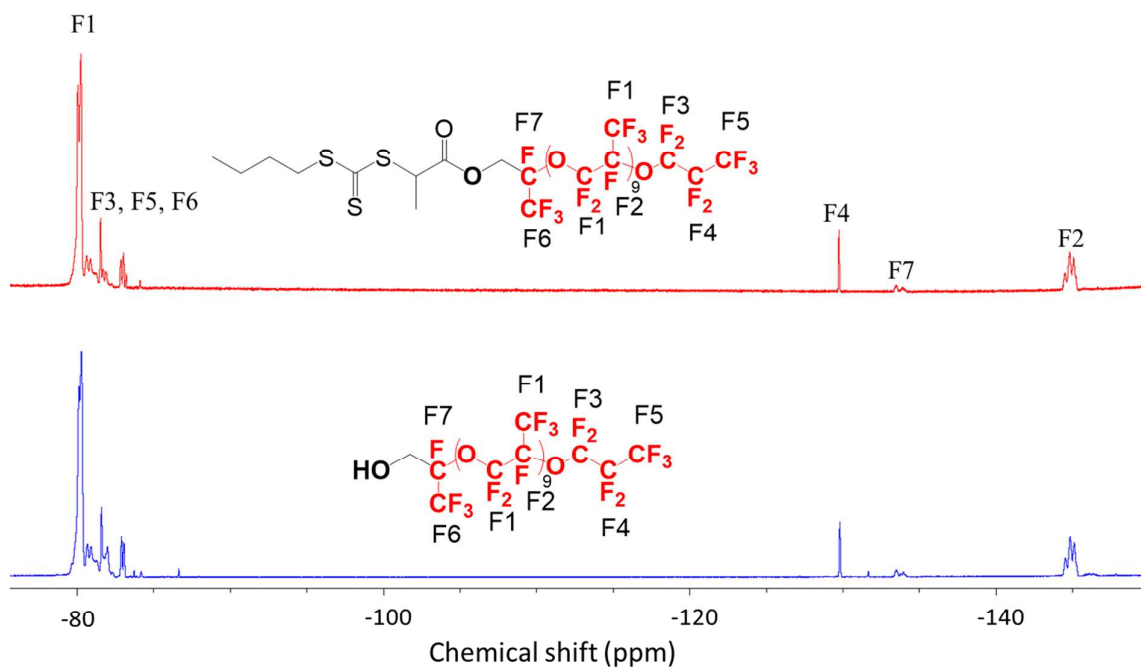


**Figure S2.** The  $^{19}\text{F}$  NMR spectrum of PFPE-OH and PABTC-PFPE macro-CTA in  $\text{CDCl}_3$ .

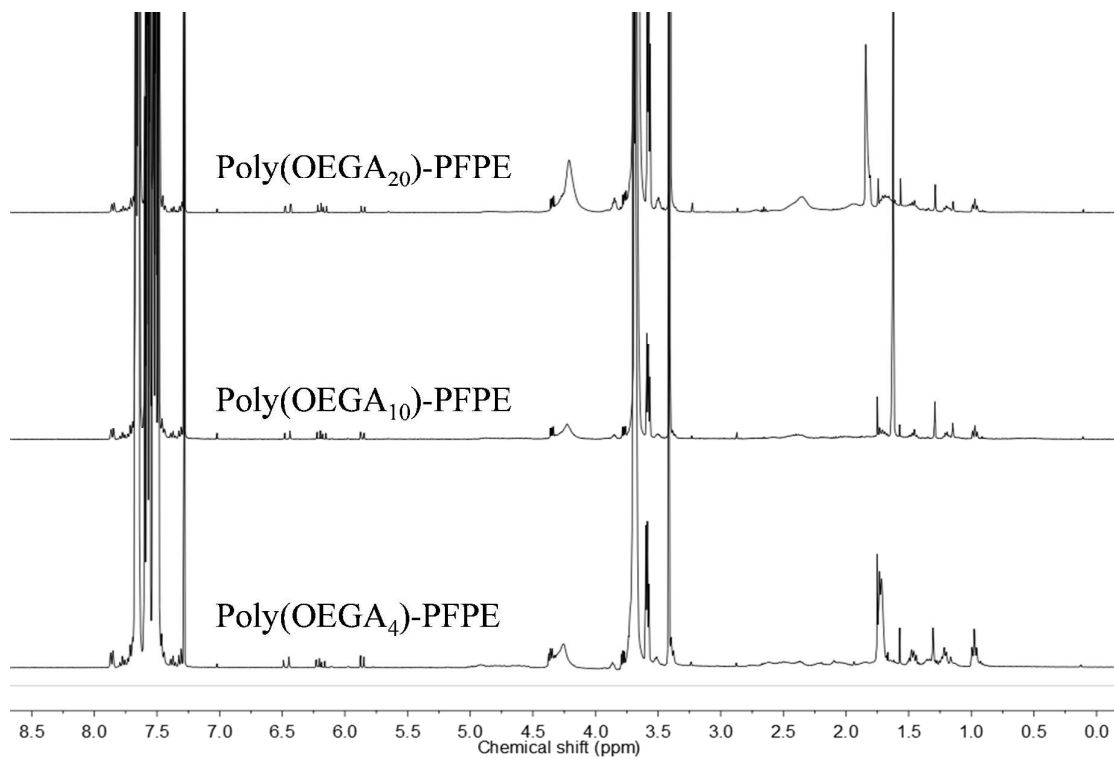


**Figure S3.**  $^1\text{H}$  NMR spectra of the crude poly(OEGA)<sub>m</sub>-PFPE polymers in  $\text{CDCl}_3$ . OEGA monomer conversion was 88.0, 89.4 and 97.2 % for poly(OEGA)<sub>4</sub>-PFPE, poly(OEGA)<sub>10</sub>-PFPE and poly(OEGA)<sub>20</sub>-PFPE, respectively.

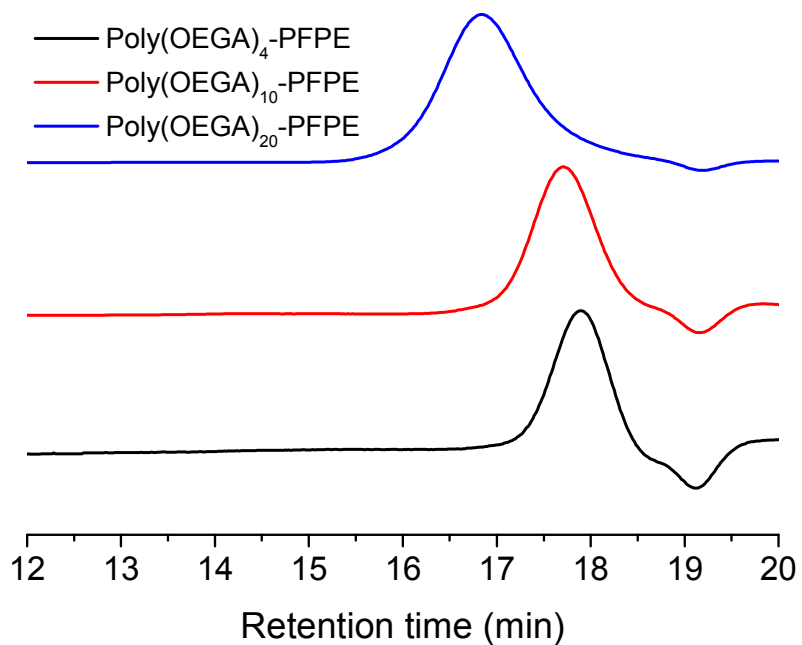


**Figure S4.** SEC chromatograms of the PFPE-based polymers obtained by RAFT polymerization. THF was used as the eluent.

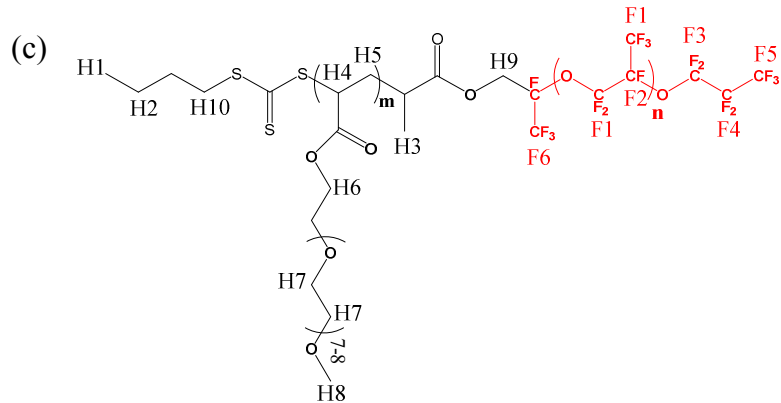
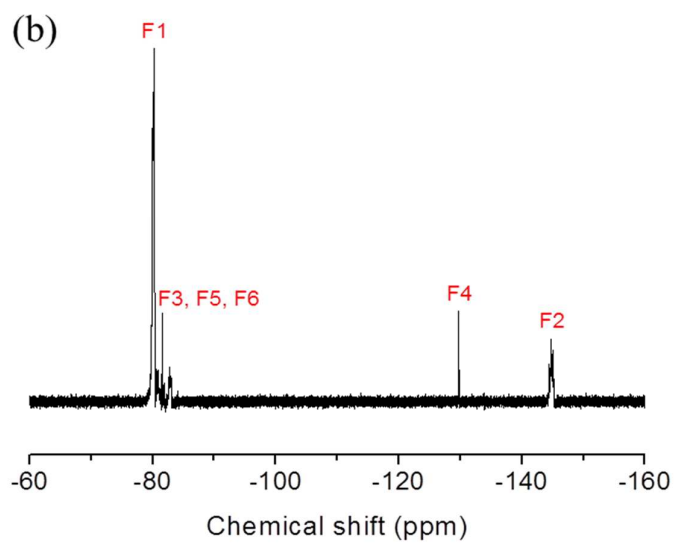
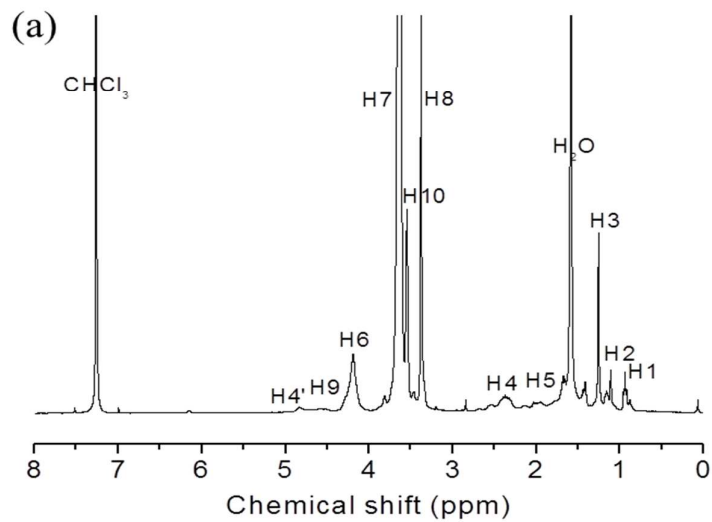


**Figure S5.** (a) and (b) The  $^1\text{H}$  and  $^{19}\text{F}$  NMR spectra in  $\text{CDCl}_3$  and assignments to the spectra of poly(OEGA<sub>10</sub>)-PFPE. (c) The chemical structure of the poly(OEGA<sub>10</sub>)-PFPE synthesized through RAFT polymerisation.

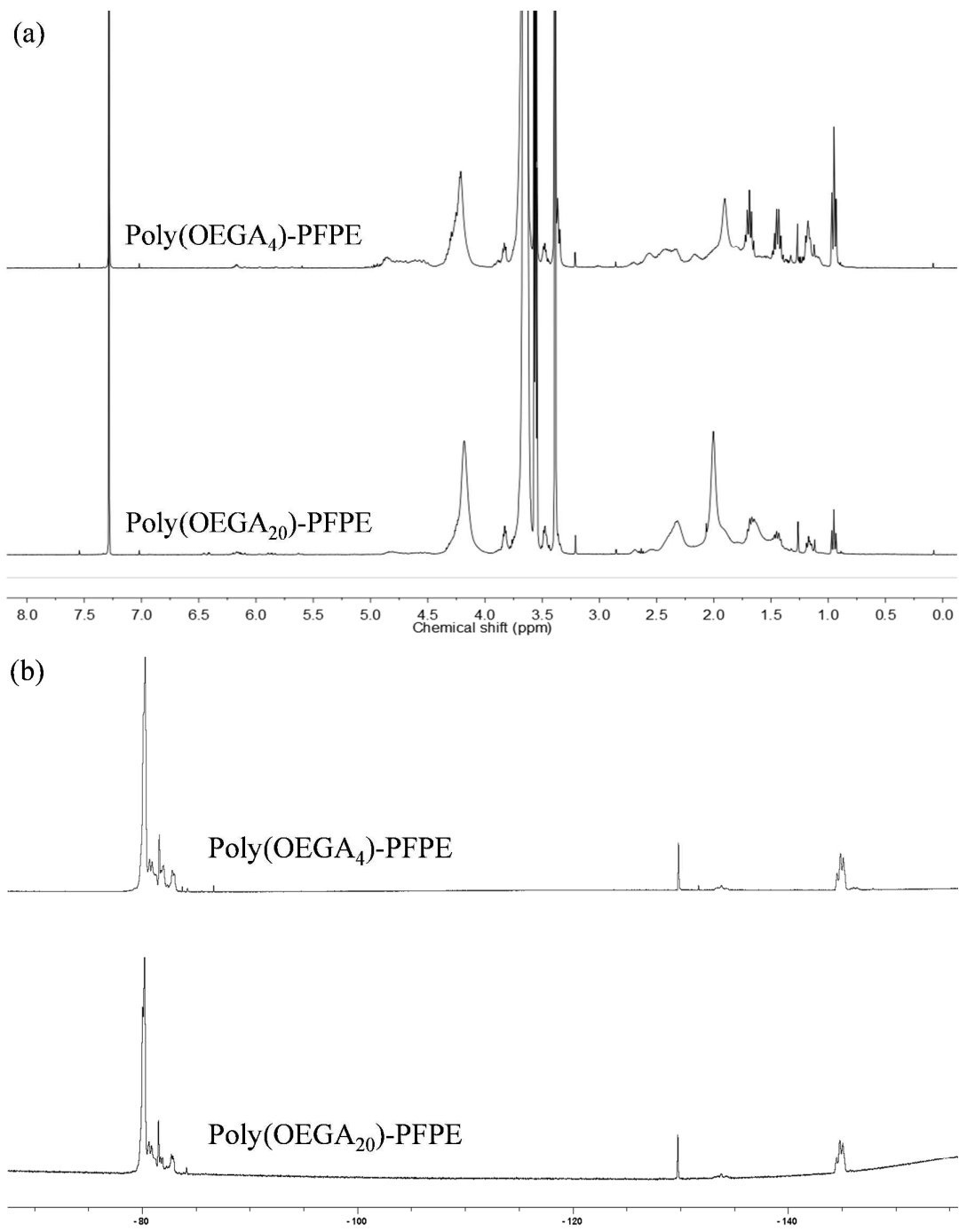


**Figure S6.** The (a) <sup>1</sup>H and (b) <sup>19</sup>F NMR spectra of the poly(OEGA)<sub>4</sub>-PFPE and poly(OEGA)<sub>20</sub>-PFPE polymers in CDCl<sub>3</sub>.

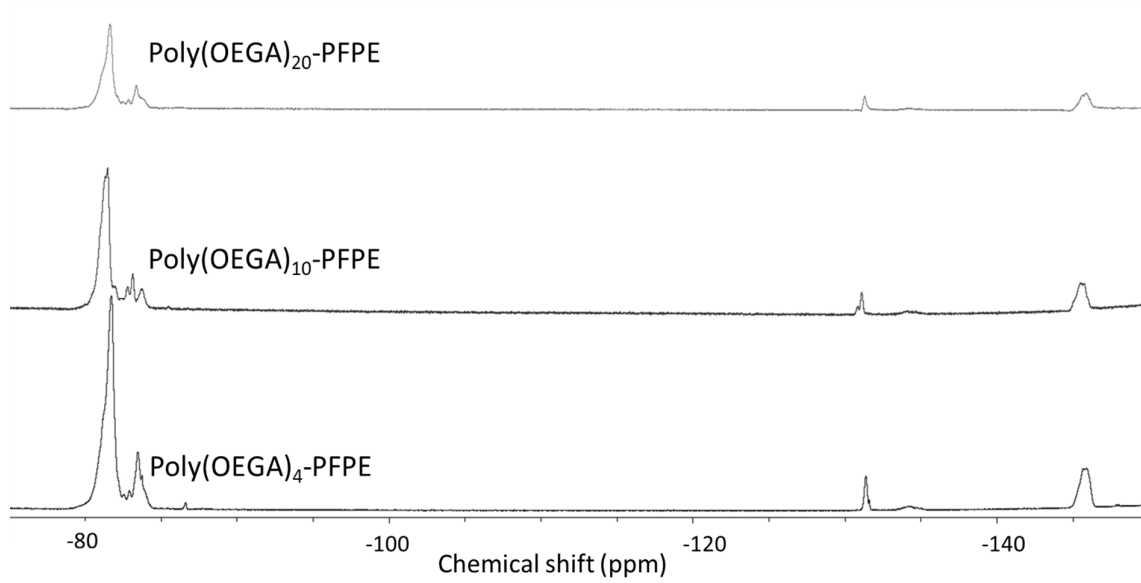


**Figure S7.**  $^{19}\text{F}$  NMR spectra of the PFPE-based polymers in PBS/D<sub>2</sub>O (V/V 90/10) at a concentration of 20 mg/mL.

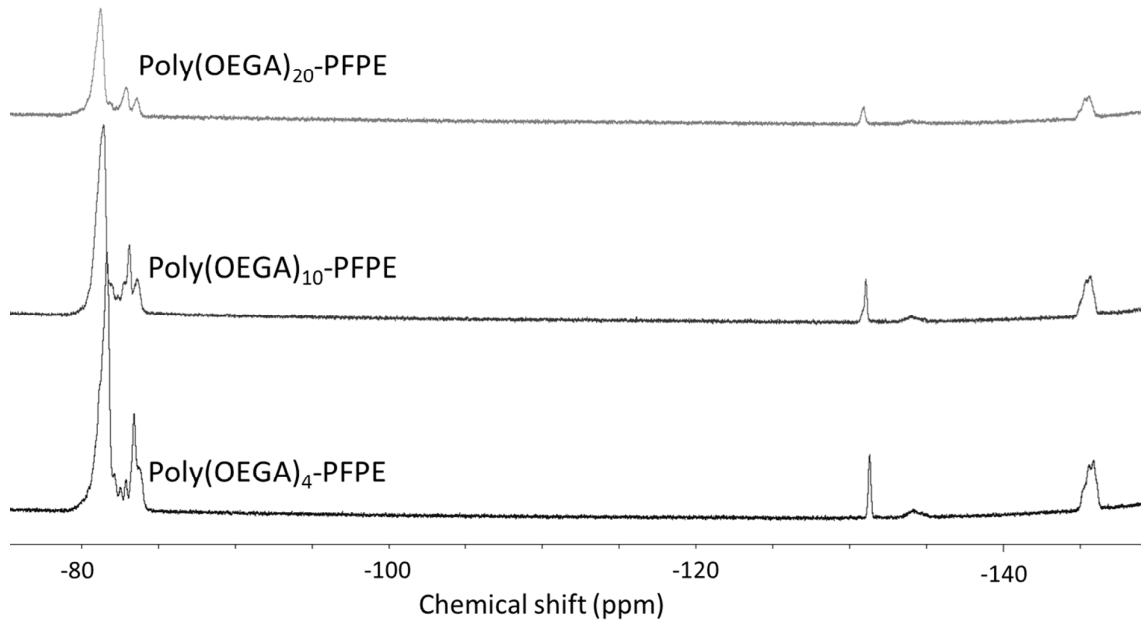


**Figure S8.**  $^{19}\text{F}$  NMR spectra of the PFPE-terminated polymers in the presence of serum (10 %).

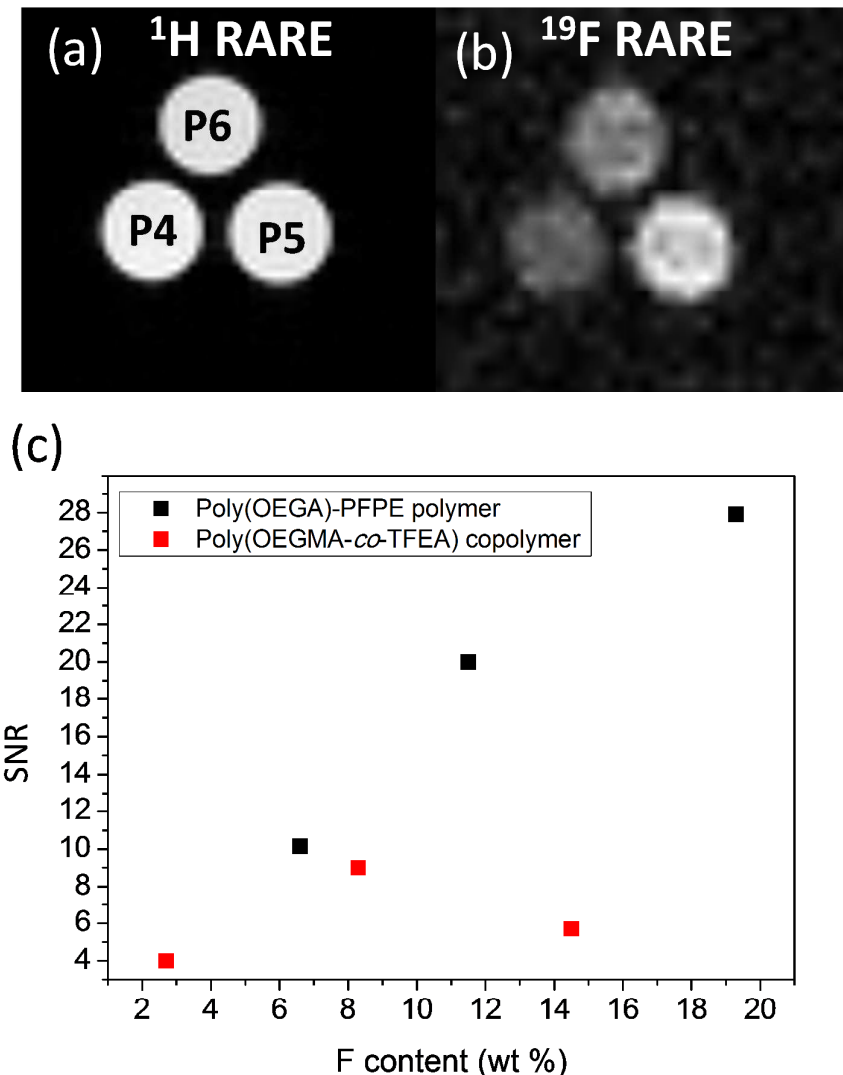


**Figure S9.** *In vitro* MR spin-echo images of the poly(OEGMA-*co*-TFEA) polymers in PBS at 20 mg/mL: (a) and (b)  $^1\text{H}$  and  $^{19}\text{F}$  RARE images. (c) The signal-to-noise ratio (SNR) obtained from the  $^{19}\text{F}$  MR images of the PFPE-based (filled black symbols) and poly(OEGMA-*co*-TFEA) polymers (filled red symbols) with different fluorine contents.

**Table S1.** The detailed structural characteristics of the poly(OEGMA-*co*-TFEA) polymers.

Data are expressed as mean  $\pm$  SD (n=3).

		Conversion OEGMA TFEA (%)	Fluorine content <sup>a</sup> (wt %)	$M_{n,\text{SEC}}^b$ (g/mol)	$M_{n,\text{NMR}}^c$ (g/mol)	$D_M^b$	$D_h^d$ (nm)
P4	Poly(OEGMA <sub>40</sub> - <i>co</i> -TFEA <sub>10</sub> )	92.6 83.3	2.7	11870	20800	1.13	4.8 $\pm$ 0.2
P5	Poly(OEGMA <sub>14</sub> - <i>co</i> -TFEA <sub>13</sub> )	78.3 52.2	8.3	7380	8900	1.17	9.6 $\pm$ 0.3
P6	Poly(OEGMA <sub>11</sub> - <i>co</i> -TFEA <sub>23</sub> )	84.5 58.4	14.5	5400	9000	1.15	36.5 $\pm$ 0.4

<sup>a</sup>the weight percentage of fluorine in the samples. <sup>b</sup> $M_{n,\text{SEC}}$  and  $D_M$  were acquired by SEC RI detector. <sup>c</sup>The calculations for the poly(OEGMA-*co*-TFEA) were reported in our previous publications.<sup>9</sup> <sup>d</sup> $D_h$  was obtained by DLS in water and based on the number-average values.

**Table S2.** NMR and MRI properties of poly(OEGMA-*co*-TFEA) in PBS. Data are expressed as mean  $\pm$  SD (n=3).

Samples	Fluorine content (wt%)	$^{19}\text{F}$ NMR T <sub>1</sub> /T <sub>2</sub> (ms) <sup>a</sup>	$^{19}\text{F}$ concentration (M) <sup>b</sup>	Image SNR <sup>c</sup>
Poly(OEGMA <sub>40</sub> - <i>co</i> -TFEA <sub>10</sub> )	2.7	484.2/152.1	0.028	4.0 $\pm$ 0.25
Poly(OEGMA <sub>14</sub> - <i>co</i> -TFEA <sub>13</sub> )	8.3	440.5/80.8	0.087	9.0 $\pm$ 0.29
Poly(OEGMA <sub>11</sub> - <i>co</i> -TFEA <sub>23</sub> )	14.5	441.3/46.8	0.15	5.7 $\pm$ 0.32

<sup>a</sup>The  $^{19}\text{F}$  NMR T<sub>1</sub>/T<sub>2</sub> were tested in PBS/D<sub>2</sub>O (90/10, v/v) at 310 K. <sup>b</sup> The  $^{19}\text{F}$  concentration of the polymers in PBS solutions. <sup>c</sup> The image SNR was calculated from the  $^{19}\text{F}$  MRI images.

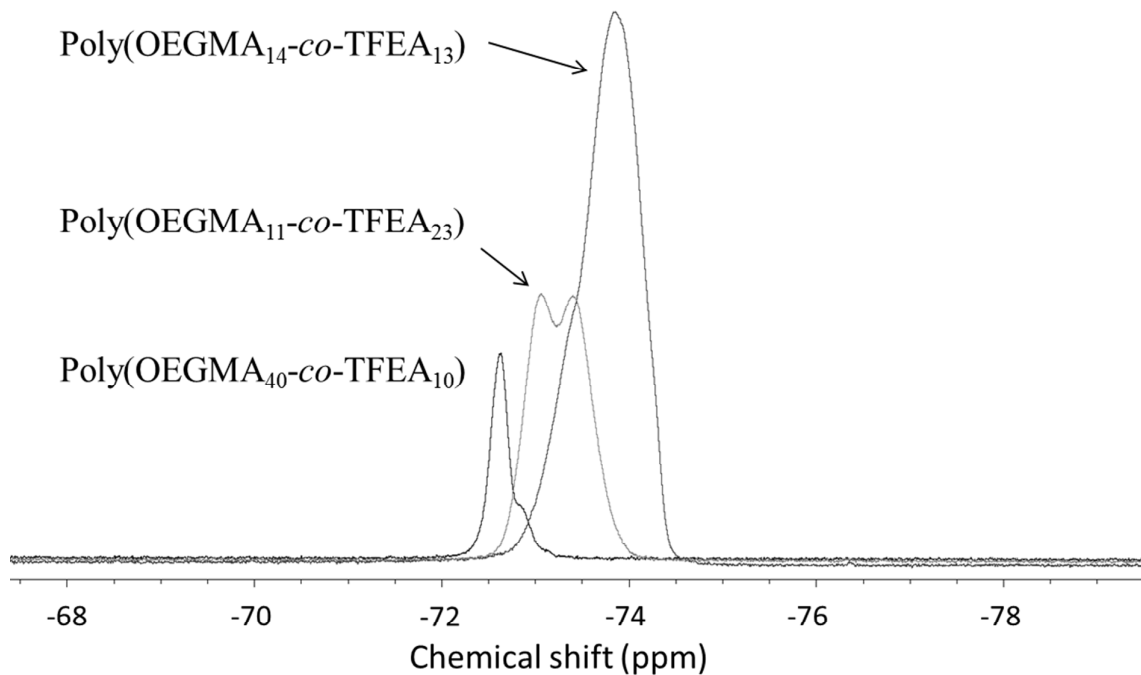


**Figure S10.**  $^{19}\text{F}$  NMR spectra of the poly(OEGMA-*co*-TFEA) copolymers.

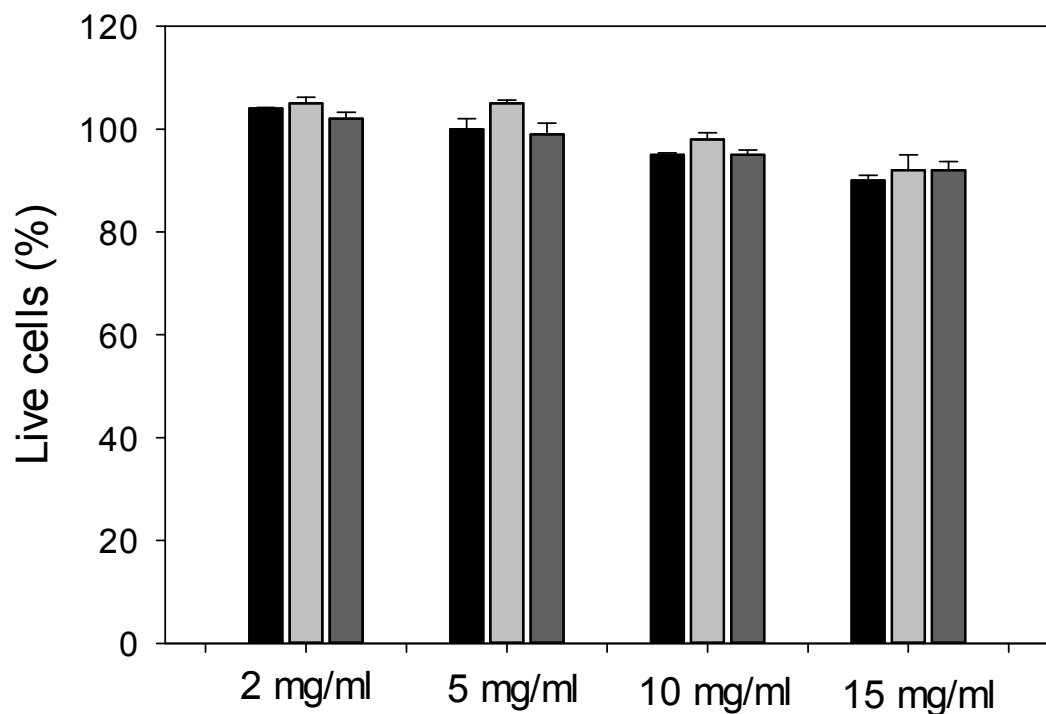


**Figure S11.** Viability of MCF-7 cancer cells after incubation with P1, P2 and P3 polymers at different concentrations for 24 h. The results are the average of three replicates  $\pm$  standard deviation.

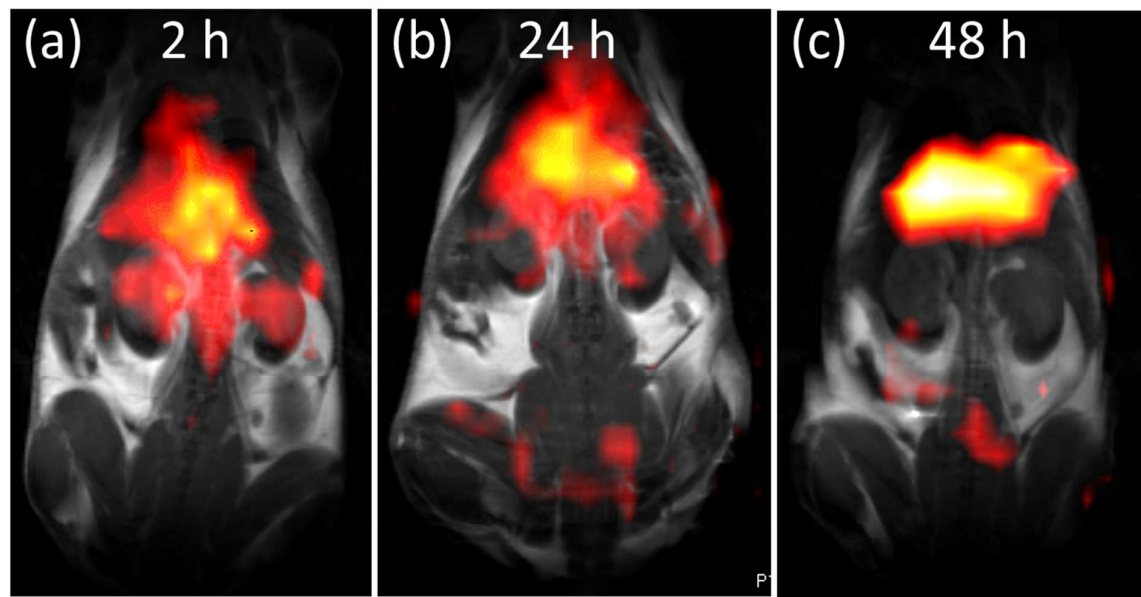


**Figure S12.** *In vivo*  $^1\text{H}/^{19}\text{F}$  MRI of the poly(OEGA)<sub>4</sub>-PFPE in mouse on a 9.4 T MRI scanner.  
(a) 2h, (b) 24 h and (c) 48 h after intravenous injection.

## REFERENCES

1. Ferguson, C. J.; Hughes, R. J.; Nguyen, D.; Pham, B. T. T.; Gilbert, R. G.; Serelis, A. K.; Such, C. H.; Hawkett, B. S. Ab Initio Emulsion Polymerization by RAFT-Controlled Self-Assembly. *Macromolecules* **2005**, *38*, 2191-2204.
2. Thang, S. H.; Chong, Y. K.; Mayadunne, R. T. A.; Moad, G.; Rizzardo, E. A novel synthesis of functional dithioesters, dithiocarbamates, xanthates and trithiocarbonates. *Tetrahedron Lett.* **1999**, *40*, 2435-2438.
3. Phillips, J. C.; Braun, R.; Wang, W.; Gumbart, J.; Tajkhorshid, E.; Villa, E.; Chipot, C.; Skell, R. D.; Kale, L.; Schulten, K., Scalable molecular dynamics with NAMD. *Journal of Computational Chemistry* **2005**, *26*, 1781-1802.
4. Vanommeslaeghe, K.; Hatcher, E.; Acharya, C.; Kundu, S.; Zhong, S.; Shim, J.; Darian, E.; Guvench, O.; Lopes, P.; Vorobyov, I.; MacKerell, A. D. J., CHARMM general force field: A force field for drug-like molecules compatible with the CHARMM all-atom additive biological force fields. *J. Comput. Chem.* **2010**, *31*, 671-690.
5. Vanommeslaeghe, K.; MacKerell Jr, A. D., Automation of the CHARMM General Force Field (CGenFF) I: Bond Perception and Atom Typing. *J. Chem. Inf. Model.* **2012**, *52*, 3144-3154.
6. Vanommeslaeghe, K.; Raman, E. P.; MacKerell Jr, A. D., Automation of the CHARMM General Force Field (CGenFF) II: Assignment of Bonded Parameters and Partial Atomic Charges. *J. Chem. Inf. Model.* **2012**, *52*, 3155-3168.
7. Yu, W.; He, X.; Vanommeslaeghe, K.; MacKerell Jr, A. D., Extension of the CHARMM general force field to sulfonyl-containing compounds and its utility in biomolecular simulations. *J. Comput. Chem.* **2012**, *33*, 2451-2468.

8. Darden, T.; York, D.; Pedersen, L., Particle mesh Ewald: An  $N \cdot \log(N)$  method for Ewald sums in large systems. *J. Chem. Phys.* **1993**, 98, 10089-10092.
9. Zhang, C.; Peng, H.; Whittaker, A. K. NMR investigation of effect of dissolved salts on the thermoresponsive behavior of oligo(ethylene glycol)-methacrylate-based polymers. *J. Polym. Sci., Part A: Polym. Chem.* **2014**, 52, 2375-2385.
10. Humphrey, W.; Dalke, A.; Schulten, K., VMD - Visual Molecular Dynamics, *J. Molec. Graphics*, **1996**, 14, 33-38.